HHS Public Access

Author manuscript

Brain Stimul. Author manuscript; available in PMC 2017 May 01.

Published in final edited form as:

Brain Stimul. 2016 ; 9(3): 406–414. doi:10.1016/j.brs.2016.02.006.

Repetitive transcranial magnetic stimulation educes frequency-specific causal relationships in the motor network

Felipe S. Salinas[1,*], **Crystal Franklin**[1], **Shalini Narayana**[2], **C. Ákos Szabó**[3], and **Peter T. Fox**[1]

[1]Research Imaging Institute, University of Texas Health Science Center at San Antonio, San Antonio, Texas

[2]Department of Pediatrics, University of Tennessee Health Science Center, Memphis, Tennessee

[3]Department of Neurology, University of Texas Health Science Center at San Antonio, San Antonio, Texas

Abstract

Background—Repetitive transcranial magnetic stimulation (rTMS) has the potential to treat brain disorders by modulating the activity of disease-specific brain networks, yet the rTMS frequencies used are delivered in a binary fashion—excitatory (> 1 Hz) and inhibitory (≤1 Hz).

Objective—To assess the effective connectivity of the motor network at different rTMS stimulation rates during positron-emission tomography (PET) and confirm that not all excitatory rTMS frequencies act on the motor network in the same manner.

Methods—We delivered image-guided, supra-threshold rTMS at 3 Hz, 5 Hz, 10 Hz, 15 Hz and rest (in separate randomized sessions) to the primary motor cortex (M1) of the lightly anesthetized baboon during PET imaging. Each rTMS/PET session was analyzed using normalized cerebral blood flow (CBF) measurements. Path analysis—using structural equation modeling (SEM)—was employed to determine the effective connectivity of the motor network at all rTMS frequencies. Once determined, the final model of the motor network was used to assess any differences in effective connectivity at each rTMS frequency.

Results—The exploratory SEM produced a very well fitting final network model (χ^2 = 18.04, *df* = 21, RMSEA = 0.000, p = 0.647, TLI = 1.12) using seven nodes of the motor network. 5 Hz rTMS produced the strongest path coefficients in four of the seven connections, suggesting that this frequency is the optimal rTMS frequency for stimulation the motor network (as a whole), however, the premotor → cerebellum connection was optimally stimulated at 10 Hz rTMS and the supplementary motor area → caudate connection was optimally driven at 15 Hz rTMS.

Conclusion(s)—We have demonstrated that 1) 5 Hz rTMS revealed the strongest path coefficients (i.e. causal influence) on the nodes of the motor network, 2) stimulation at

[*]Correspondence to: salinasf@uthscsa.edu.
Permanent address: 8403 Floyd Curl, San Antonio, TX, USA 78229

"excitatory" rTMS frequencies did not produce increased CBF in all nodes of the motor network, 3) specific rTMS frequencies may be used to target specific none-to-node interactions in the stimulated brain network, and 4) more research needs to be performed to determine the optimum frequency for each brain circuit and/or node.

Keywords

TMS; PET; effective connectivity; motor cortex; rate; network

INTRODUCTION

Repetitive transcranial magnetic stimulation (rTMS) has the potential to treat brain disorders by modulating the activity of disease-specific brain networks. A prime example of this approach may be seen in the rTMS treatments of the fronto-limbic network of major depressive disorder,[1–3] in which rTMS is delivered to the dorsolateral prefrontal cortex to indirectly modulate the activity levels of the subgenual cingulate—which is too deep for standard rTMS coils to reach. Traditionally, rTMS rate has been applied in rTMS treatment protocols in either an inhibitory (≤1 Hz) or excitatory (>1 Hz) fashion,[4,5] where it is assumed that these inhibitory or excitatory rTMS treatments affect the targeted brain networks in the same linear way—i.e. excitatory brain activity at the target site produces excitatory brain activity at all of the remote sites of the network.[6,7]

In our previous study,[8] we reported that a unimodal relationship (peaking at 5 Hz rTMS) existed between rTMS frequency and the cerebral blood flow (CBF) of the motor network during concurrent positron emission tomographic (PET) imaging. We also found that some of the nodes in the motor network were maximally inhibited at 5 Hz rTMS. Therefore, it is not appropriate to assume: 1) that increasing rTMS frequency will result in higher levels of brain activity or 2) that high rTMS frequencies (e.g. > 1 Hz) will produce excitatory brain activity in all nodes of the targeted brain network. In this study, we extend our previous results[8,9] by investigating the effective connectivity of the baboon's motor network—at different rTMS frequencies—to determine if 5 Hz rTMS is the optimal frequency for stimulation of all of the nodes within the motor network.

MATERIALS & METHODS

Animal preparation

Five healthy, adult baboons (*Papio hamadryas anubis;* 4 females; age = 11.61 ± 2.92 years (mean ± SEM); body weight = 17.50 ± 5.42 kg) were studied in accordance with the policies of the Institutional Animal Care and Use Committee of the University of Texas Health Science Center at San Antonio; this study fully complied with U.S. Public Health Service's *Guide for the Care and Use of Laboratory Animals*[10] and the *Animal Welfare Act*.[11] The data acquired in these five animals was used in prior publications[8,9]; the results from these prior publications were reanalyzed in this study to assess the effective connectivity of the baboon's motor network. Each animal was pre-screened—using electroencephalography[12]—to ensure that only animals with no neurological deficits were enrolled in the study. The optimized anesthetized animal preparation has been described in

previous studies.[9,13] Each animal received an injection of intramuscular ketamine (5 mg/kg) and atropine (0.3 mg) before each MRI and PET imaging procedure. We maintained sedation during each imaging session with continuous *i.v.* administration of ketamine (5–6 mg/kg/hr) and a paralytic (vecuronium; 0.25 mg/kg/hr). Upon conclusion of the imaging session, we administered atropine (0.6–1.2 mg, *i.v.*) and neostigmine (0.5–2.0 mg, *i.v.*) to reverse muscle paralysis. During the entire procedure, the animals' respiration, heart rate and oxygenation were monitored.

Magnetic Resonance Imaging

All MRIs were performed on a Siemens TIM-Trio 3T clinical scanner using a body radiofrequency (RF) transmission coil with a 12-channel head RF receiver coil (Siemens, Erlangen, Germany). We obtained high-resolution anatomical images using an MP-RAGE sequence (TR/TE/flip angle = 2300 ms/3.66 ms/13°) with slice-select inversion recovery pulses (TI = 751 ms), FOV = 128 mm × 128 mm × 80 mm, and 0.5 mm isotropic spatial resolution. We used the anatomical MRIs for co-registration between imaging modalities (MRI and PET) in order to register each animal's $H_2{}^{15}O$ PET images to their native MRI then warp them to a representative baboon's MRI brain space.

Blood-oxygen-level dependent (BOLD) fMRI was acquired using gradient-echo, echo-planar imaging (EPI; TR/TE = 2.5 s/30 ms), FOV = 150 mm × 150 mm x 48 mm, and spatial resolutions of 1.5 mm × 1.5 mm × 4 mm. Somatosensory stimulation was applied to the animal's right hand via a custom-made pneumatic-driven vibrotactile stimulator;[13] vibrotactile stimulations were applied—at a stimulation frequency of 5 Hz—using an 50 second on/off block design. We processed the fMRI data using the FEAT toolbox[14] in the FMRIB's Software Library (FSL).[15] The resulting fMRIs were utilized to determine the location of each baboon's primary sensory cortex representation of the right hand ($S1_{hand}$). The $S1_{hand}$ and primary motor cortex representation of the hand ($M1_{hand}$) representations lie directly across the central sulcus from one another.[16] Therefore we determined each animal's $M1_{hand}$ location (i.e. target location) to be the site in the precentral gyrus, which is adjacent to that animal's $S1_{hand}$ fMRI activation. We validated this approach in our previous baboon TMS/PET study.[9]

rTMS

All TMS delivery was image-guided, using high-resolution structural and functional magnetic resonance images (fMRIs) using previously described techniques.[9,13] We used a MagPro Cool-B65 figure-of-eight rTMS coil connected to a MagPro R30 Magnetic Stimulation Unit (MagVenture A/S, Farum, Denmark) for each rTMS procedure. The TMS coil's site of maximal electric field (E-field) induction (i.e. "hot spot") was determined using methods developed by Salinas *et al.*[17,18] Using each animal's fMRI map of the $S1_{hand}$ and the corresponding target locations for $M1_{hand}$, we determined the scalp location closest to the $M1_{hand}$ site, then measured the distances from this scalp location to specific anatomical landmarks (nasion, inion, earholes). Finally, we stereotactically positioned the TMS coil over each animal's left primary motor cortex ($M1_{hand}$), while lying supine in the PET scanner, so that the location of the TMS coil's maximum induced E-field coincided with the targeted M1 location. Once positioned, the orientation of the TMS coil—i.e. the E-field and

current direction—was adjusted to be perpendicular to the animal's central sulcus (with the E-field directed antero-medially, towards the animal's snout); this approach is consistent with the cortical column cosine (C3) aiming theory proposed by Fox *et al.*.[19] We applied single pulses of TMS to each baboon's left $M1_{hand}$ to visually establish each animal's resting motor threshold (rMT) at the first dorsal interosseous (FDI) muscle of the contralateral hand; the rMT was defined as the minimum intensity of stimulation capable of producing FDI muscle contractions in at least 5 out of 10 trials. Once each baboon's rMT was found, a one-time bolus injection of vecuronium was given to eliminate movement throughout the rTMS/PET session.

Each baboon underwent rTMS at stimulation frequencies of 3 Hz, 5 Hz, 10 Hz and 15 Hz. rTMS pulses were delivered to $M1_{hand}$ at 120% rMT during concurrent $H_2{}^{15}O$ PET scans. Each rTMS frequency was delivered at least 30 seconds prior to the injection of ^{15}O-labeled water and continued until 60 seconds after the injection. The number of rTMS pulses delivered at each stimulation frequency was held constant at 450 pulses (e.g. train duration varied across frequencies); this was done to decrease any possible dose effects—which may alter the excitability state of the motor cortex.[20,21,22] The 3 Hz rTMS frequency was continuously applied 90 seconds prior to radiotracer injection and continued for 60 seconds afterward, for a total 3 Hz rTMS duration of 150 seconds. The 5 Hz rTMS frequency was also continuously applied, but began only 30 seconds prior to radiotracer injection and continued for 60 seconds afterward, for a total 5 Hz rTMS duration of 90 seconds. The 10 Hz rTMS frequency was applied intermittently in 5 second trains with 5 second inter-train intervals, whereas the 15 Hz rTMS frequency was applied intermittently in 5 second trains with 10 second inter-train intervals; the 10 Hz and 15 Hz rTMS pulse trains began 30 seconds prior to radiotracer injection and continued for 60 seconds, for a total rTMS duration of 90 seconds (e.g. 450 pulses for each rTMS frequency). The order of stimulation frequencies was randomized and a rest condition was used to represent the baseline scan.

Electroencephalography

We performed EEG recordings throughout each rTMS/PET session to monitor the level of sedation and any possible onset of seizure activity. The EEG unit used in this study was not TMS-compatible therefore we did not analyze the resulting EEG waveforms for real-time TMS-induced effects. After the baboons were sedated, we positioned eight cephalic electrodes for each rTMS session (FP1, FP2, T3, C4, O1, O2, ground and reference sites)—using the 10–20 EEG system—with EEG electrode paste and secured them with collodion-soaked gauze strips. The electrodes were connected to a portable, laptop-based EEG acquisition machine (Nihon-Kohden, Tokyo, Japan), which enabled real-time monitoring of the EEG waveforms (when the signal was not contaminated by rTMS artifacts); in addition to online EEG monitoring, the EEG results of each rTMS/PET session were also reviewed by a board-certified clinical neurophysiologist (C.Á.S.).

Positron emission tomography

PET data were acquired with a CTI EXACT HR+ scanner (Knoxville, TN). Sixty-three contiguous slices (2.5 mm thick) were acquired in a transaxial plane of 128 x 128 voxels with a 2 mm in-plane voxel resolution. Images were corrected by measured attenuation

using 68Ge/68Ga transmission scans and reconstructed at an in-plane resolution of 7-mm full width at half maximum (FWHM) and an axial resolution of 6.5-mm FWHM. Water labeled with oxygen-15 ($H_2{}^{15}O$, half-life of 122 s) was administered intravenously—370 MBq $H_2{}^{15}O$ dose/scan—and cerebral blood flow (CBF) was measured using a bolus technique.[19] We applied each condition (high-frequency rTMS or rest) once during each PET session. We immobilized each baboon in the PET scanner using a custom-made, padded animal restraint.[9]

Data analysis

We performed image preprocessing using previously validated methods and in-house software.[19] PET images were reconstructed into 60 slices (2 mm thick) with an image matrix size of 60 x 128 x 128, using a 5 mm Hann filter resulting in images with a spatial resolution of approximately 7 mm (full-width at half-maximum (FWHM)). PET images were corrected for head motion using the MCFLIRT tool[23] in FSL; the PET and MRI images were spatially transformed to a representative baboon's MRI brain space and co-registered using the Convex Hull algorithm.[24] Regional tissue uptake of ^{15}O-water was value normalized to a whole-brain (global) mean of 1000 counts.

Structural Equation Modeling

Cubic regions of interest (ROIs; 3 mm x 3 mm x 3 mm) were selected from the statistical parametric imaging results of the "All rTMS vs. Rest" experiment presented in Salinas *et al.,*[8] which demonstrated the highest levels of brain activity during rTMS while targeting the motor cortex (Figure 1). These regions included the: targeted dorsal precentral (L-M1), ipsilateral dorsal premotor (L-PM), supplementary motor area (SMA), contralateral anterior cingulate (R-Cg), contralateral cerebellum (R-Cb), ipsilateral caudate (L-Cd), contralateral thalamus (R-Th), ipsilateral parietal operculum (L-SII), ipsilateral insula (L-Ins), and contralateral anterior intraparietal sulcus (R-AIP). We also included an ROI for the contralateral dorsal precentral (R-M1) gyrus since it has been reported to demonstrate decreased CBF during low-frequency (i.e. ≤1Hz) rTMS to L-M1.[4,20,25–27] The coordinates and relative cerebral blood flow strengths of each of these regions are listed in Table 1; the labels associated with these regions correspond to homologous areas in the rhesus brain.[28]

Each subject's average normalized PET counts were obtained for each ROI at: rest, 3 Hz rTMS, 5 Hz rTMS, 10 Hz rTMS, and 15 Hz rTMS. These ROI datasets were input to Amos 7.0[29] for structural equation modeling (SEM) of rTMS frequency in the motor network in a step-wise, exploratory search. The exploratory search used in this analysis replicated that of Laird *et al.*,[30] which used SEM to assess the effect of TMS intensity on the human motor network. In our approach, each ROI was modeled as an observed, endogenous variable while a separate observed, exogenous variable—which directly modulated the stimulated site—was also modeled (e.g. rTMS rate in our study).[8] Error terms (loaded onto each ROI) were also modeled as unobserved, exogenous variables.

We used path analysis—a subset of SEM—to determine the baboon's optimal SEM of the motor network. This procedure began by assuming that rTMS rate acted unidirectionally at the site of stimulation—i.e. L-M1. From this initial path, we used a specification search,

which assumes that the L-M1 site may (unidirectionally) propagate to each of the other ten ROIs; for a description of the procedure see Figure 2. Each stepwise search records which path has the best fit (according to the data) then adds or removes one optional path at a time until the model cannot be improved. If at any point, one of the paths had any potential alternate connections, then a separate model of the network was created and assessed using the Bayes information criterion (BIC) and Browne–Cudeck criterion (zero-scale) (BCC). Path models with the lowest (i.e. closest to zero) BIC and BCC values were selected as the model that represented the optimal model relative to the actual data. The BIC and BCC are predictive fit indices that are used to rank competing SEM models that are fit using the same data. Once determined, the second-level pathway's node(s) propagated to each of the other ROIs until an optimized third-level path was determined. This process continued until further iterations ceased to yield any new paths. To assess goodness-of-fit we utilized the: chi-square (χ^2) statistic, the root-mean-square error of approximation (RMSEA), and the Tucker-Lewis index (TLI). In general, models with the following ranges of parameters are acceptable: an insignificant χ^2 value, an RMSEA value of less than 0.08, and a TLI > 0.95; each fit characteristic and their ranges are thoroughly described in Laird et al..[30] Of all of the potential SEM models created during path analysis, an optimal SEM model was chosen based on its BCC and BIC values as well as its χ^2, RMSEA, and TLI goodness-of-fit statistics. Once established, this optimal SEM model was then used to assess rTMS frequency-specific differences on the node-to-node effective connectivity in the motor network. To ensure that any potential outliers within our PET dataset did not skew these results, we also ran the path analysis and frequency comparison steps five separate times—with each iteration excluding a different subject's data from the analysis.

RESULTS

As we stated in our previous reports,[8,9] we observed no adverse rTMS-induced effects during or immediately following each animal's rTMS/PET session. Within one hour of each rTMS/PET session, each animal recovered from their lightly sedated state and began exhibiting normal behavior and activity levels.

Structural Equation Modeling

The rTMS/PET study consisted of 25 data points (5 animals x 5 conditions). The final SEM modeled 25 variables: 7 observed, endogenous variables for each ROI, 7 unobserved, exogenous variables for the error terms loaded onto each ROI, and 1 observed, exogenous variable for rTMS rate. Beginning with the required path of rTMS rate loading onto L-M1, we then assessed which of the possible first-level paths (Figure 3, red path) would exist from L-M1 to the six other potential ROIs (i.e. nodes). From the site of stimulation (i.e. L-M1), a specification search revealed that rTMS-induced brain activity spread the to ipsilateral premotor cortex.

In the second-level of path analysis, the first-level path from L-MI to ipsilateral premotor cortex was set as required and six optional path loadings were drawn from the ipsilateral premotor cortex to all of the other nodes (including an optional feedback path to L-M1). Three second-level paths survived this level of the analysis resulting in second-level path

loadings from the ipsilateral premotor cortex to the ipsilateral insular cortex, SMA, and the contralateral cerebellum (Figure 3, blue paths).

In the third-level of path analysis, the first and second-level paths were set as required and eighteen optional path loadings (3 ROIs x 6 nodes) were drawn from the ipsilateral insular cortex, SMA, and the contralateral cerebellum to all other nodes. Two third-level paths survived, resulting in third-level path loadings from: 1) the SMA to the ipsilateral caudate nucleus and 2) the contralateral cerebellum to the R-M1 (Figure 3, green paths). A fourth-level path analysis with the respective optional loadings indicated that the current three-level model would not be improved by adding more path levels. The final model of the baboon's L-M1 connectivity is shown in Figure 3.

The exploratory SEM produced a very well fitting final network model ($\chi^2 = 18.04$, $df = 21$, RMSEA = 0.000, p = 0.647, TLI = 1.12) using only 7 of the initial 11 ROIs. Other SEM models created during the specification search procedure did not meet our selection criteria (described in "Structural Equation Modeling" of the Methods section). The four nodes excluded from the final model were the contralateral anterior cingulate, contralateral thalamus, ipsilateral parietal operculum, and contralateral anterior intraparietal sulcus. The seven nodes in the final motor network model are consistent with those shown in Laird *et al.*,[30] and consisted of the L-M1, ipsilateral premotor, SMA, ipsilateral insula, contralateral cerebellum, ipsilateral caudate, and the R-M1.

The fit statistics for each level of the analysis were shown in Table 2. The χ^2 statistic may be used to assess differences between the modelled and measured covariance matrices.[30,31] The goodness of fit of the model improves (e.g. higher *p*-values) as the χ^2 value decreases. The table clearly shows that the *p*-value of each level of the model only significantly increased after the third-level paths were added to the model. Although the Browne-Cudeck criterion (BCC) and Bayes information criterion (BIC) were outstanding (i.e. 0.000) at each path level, only the *p*-value changed when path levels were added to the model—suggesting that these third-level paths play an important role in the final network model.

rTMS frequency effects on effective connectivity

Using the final model of effective connectivity in the motor network, we assessed each rTMS frequency's effect on the node-to-node interactions at each path level (Table 3). In the first-level paths—1) rTMS rate to L-M1 and 2) the L-M1 to premotor—it is clear that the relative strength of the effective connectivity of these paths increases as rTMS frequency increases from 3 Hz to 5 Hz. However, as rTMS frequency increases from 5 Hz to 15 Hz, the relative strength of the effective connectivity decreases. This unimodal trend of effective connectivity increasing to a maximum at 5 Hz rTMS then decreasing at higher rTMS frequencies was also demonstrated in the second-level paths. Specifically, the premotor to SMA path had a positive correlation with this trend whereas the premotor to insula path was negatively correlated with the unimodal trend peaking at 5 Hz rTMS. Interestingly, the premotor to cerebellum path did not follow this trend. At 5 Hz rTMS, the premotor to cerebellum path demonstrated the weakest effective connectivity, whereas 10 Hz rTMS had the strongest effective connectivity for this path. In the third-level paths, the SMA to caudate path had a bimodal distribution, peaking at 3 Hz and 15 Hz rTMS. The cerebellum to R-M1

path exhibited its strongest effective connectivity paths at the 10 Hz and 15 Hz rTMS frequencies, however none of the rTMS frequencies in this path were significantly different from rest.

Outlier Assessments

In each of the five iterations—in which we removed one animal's PET data from the path analysis (i.e. N = 4)—we obtained the same final SEM model as was found when using all five baboons, suggesting that our final SEM model is an accurate representation of the baboon's motor network. Furthermore, in each of these iterations, the frequency-specific differences in the path coefficients (found using the final SEM model) were very similar to the path coefficients found using all five baboons. As expected, due to the lower sample size of these iterations (N = 4) the *p*-values associated with each path coefficient were higher than in the full sample. These findings lead us to believe that our dataset, although small, demonstrates robust results and that these results are not due to one particular subject.

DISCUSSION

The aim of this study was to quantify the effective connectivity of the motor network during stimulation of the L-M1 hand region at various rTMS stimulation rates. Eleven ROIs (obtained using statistical parametric mapping) and rTMS rate were modeled as observed variables in the path analysis, however, only seven ROIs remained in the final version of the effective connectivity model (Figure 3). It is important to note that the four ROIs (i.e. nodes)—which were excluded from the final model—were still activated (or deactivated) during rTMS[8,9]; otherwise they would have not been chosen as ROIs in the initial SEM model. Laird *et al.*[30] found varying TMS intensity influenced the contralateral cingulate, contralateral thalamus, and ipsilateral parietal operculum nodes. When assessing the effects of varying rTMS rates, however, these nodes did not appear to be significantly affected. Thus, we may conclude that although the brain activity of these nodes is altered by supra-threshold rTMS, the effect of changing the rTMS rate did not significantly affect the way that these nodes communicate within the motor network. Also, our small sample size (N=5) may have influenced the inclusion of these nodes by increasing the statistical significance threshold for each node in the final model. Therefore, more research must be done to resolve whether or not the preliminary effective connectivity findings (described in this study) are affected by rTMS rate or if they are only influenced by increasing TMS intensity.

The effective connectivity of the seven nodes which were included in our path analysis were influenced by varying the rTMS rate, therefore these nodes comprised the final model of the rTMS rate's effect on the baboon's motor network. Interestingly, the contralateral M1 (i.e. R-M1) did not demonstrate a direct pathway to L-M1. We believe that there are two reasons for this: 1) the effect of changing rTMS rate did not affect the cortico-cortical (i.e. structural) connections between L-M1 and R-M1 and 2) the use of higher rTMS frequencies confounded the R-M1 site's CBF responses to stimulation. Many neuroimaging studies of the effects of rTMS have reported mixed results on contralateral M1 activity[20,25–27,32,33] at different rTMS frequencies and intensity ranges—specifically when rTMS is applied at low frequencies (e.g. 1 Hz). Thus, it is not very surprising that R-M1 does not have a first-level

path connection to L-M1 in the final model at the high frequencies (3–15 Hz) used in this study. Nonetheless, each of the seven ROIs used in our path analysis have consistently been reported to be functionally connected in the human[19,30,34,35] and non-human primate[36,37] motor networks.

SEM of the motor network

The final SEM model presented a very well fitting estimate (χ^2 = 18.04, *df* = 21, RMSEA = 0.000, TLI = 1.12) of the measured CBF responses induced by rTMS. This suggests that although we only had five baboons included in the analysis, their CBF responses were so robust that they could overcome SEM's statistical significance criteria even with such a small sample size. In addition, by implementing a step-wise exploratory SEM, we maximized the likelihood that the final model's pathways were informed by the measured CBF data and not the result of a hypothesis-driven approach. Thus, the nodes and paths in the final SEM model were the result of data-driven (i.e. unbiased) procedures; this approach may also have contributed to outstanding levels of fit in the final SEM model.

Frequency-specific nodal responses

In our previous publication,[8] we proposed that the motor network appeared to be maximally driven at 5 Hz rTMS. Using path analysis, we have now shown that the majority of the nodes in the motor network are optimally driven (either excitatory or inhibitory) at 5 Hz supra-threshold rTMS. This result supports our previous hypothesis[8] that a simple treatment of stimulation rate as either excitatory (> 1 Hz) or inhibitory (≤1 Hz) may be inadequate, since not all higher rTMS frequencies elicited maximized CBF responses in the motor network. In addition, our current analysis revealed that some nodes in the targeted brain network might be optimally driven at different rTMS frequencies, since some inter-nodal relationships—such as the premotor → cerebellum path—have stronger path coefficients at rTMS frequencies other than 5 Hz (Table 3). This finding may have a significant impact on the efficacy of rTMS therapies—specifically in rTMS treatments of major depressive disorder—where rTMS is used to target accessible (i.e. superficial) brain regions which (hopefully) drive the remote nodes of the affected brain circuit. If these remote brain targets are not optimally driven at an artificially determined "excitatory" (e.g. > 1 Hz) rTMS frequency than the impact of the treatment(s) may be reduced or possibly reversed since 5 Hz rTMS was also shown to be the optimal stimulation rate for inhibiting the premotor → insula pathway in the motor network.

In addition, rTMS treatment protocols targeting other nodes within the motor network (i.e. cerebellum, premotor cortex, etc.) may also be apprised by the results of this study. For example, Vasant *et al.*[38] reported that when stimulating the cerebellum with various rTMS frequencies (i.e. 1, 5, 10, and 20 Hz), only 10 Hz rTMS produced lasting effects in each subject's cortico-pharyngeal motor evoked potentials (MEPs). Recall that in this study, we demonstrated that the premotor → cerebellum connection was also optimally stimulated at 10 Hz rTMS (Table 3), suggesting that the cerebellum may prefer stimuli delivered at this frequency. Consequently, the frequency-specific path coefficients described in our M1 study, may also be used to inform rTMS practitioners of another node's *a priori* rTMS frequency preferences. Furthermore, by determining the influence of rTMS frequency in other brain

networks (e.g. the fronto-limbic circuits involved in the pathogenesis of depression[1–3,39]), we may be able to establish the preferred rTMS frequency ranges for each node of the network being stimulated. This concept has the potential to greatly impact the efficacy of neuromodulatory therapies since it suggests that specific brain circuits may be targeted not only by their anatomical location, but also by the frequency-dependence of the brain network's nodes. We believe that much work must be done on the frequency-dependence of specific brain circuits and that the information obtained from these studies may drastically improve the effect sizes (and/or remission rates) of many rTMS treatment protocols in both psychiatric and neurological disorders.

The baboon model of rTMS

We have discussed the main advantages of the baboon model of TMS in our previous publications.[8,9] One of these advantages is that we can eliminate the effects of afferent feedback to the primary motor cortex by using a muscle paralytic. At supra-threshold TMS intensities delivered to the primary motor cortex, action potentials are produced, resulting in the contraction of the targeted muscle(s). The afferent feedback produced with each muscle contraction may influence the size and/or state of the local (i.e. targeted M1) brain activity. By eliminating this feedback, we are essentially able to more directly assess the effects of rTMS on the motor network. The use of a paralytic also ensured that the animal's head (i.e. the targeted M1 site) did not move away from the stereotactically positioned TMS coil throughout the rTMS/PET session.

A second advantage of the baboon model of TMS is its potential to investigate the safety aspects of rTMS—specifically at high frequency, supra-threshold rTMS intensities. Chen *et al.*[40] investigated the effects of supra-threshold rTMS (i.e. 1–25 Hz) on the motor system and found that the safe train duration of rTMS at 120% rMT was: 10 sec at 5 Hz and 3.2 sec at 10 Hz rTMS; they did not report safe train durations for supra-threshold 15 Hz rTMS. In our study, we applied rTMS at 120% rMT at train durations of: 90 sec at 5 Hz, 5 sec at 10 Hz, and 5 sec at 15 Hz while acquiring online CBF measurements. Therefore, the baboon model of TMS enables us to assess 1) the safety limits of rTMS intensity, frequency, and duration and 2) the effects of each rTMS parameter on the targeted brain network (using either functional or effective connectivity measures).

As we have acknowledged in our previous baboon TMS studies,[8,9] the use of anesthesia in this study may diminish its informative potential, however, our research group has investigated the effects of anesthesia in many previous baboon neuroimaging studies[8,9,13,41–43] and we have found that at these relatively low doses there are no significant anesthesia effects on CBF—either globally or locally. Therefore, we are confident that the CBF responses reported in this study were the direct result of rTMS and were not due to anesthesia effects. Conversely, we could argue that low-doses of anesthesia actually made our experimental results more robust since the baboons were able to tolerate longer rTMS/PET sessions (i.e. 3 hours) than human rTMS/PET studies.[19,30,34,35] Accordingly, we understand that all rTMS effects found using our baboon model should be replicated in 1) larger sample sizes of non-human primates (with minimal to no anesthesia) and 2) human cohorts; these efforts are currently being explored by our research group.

Intermittent vs. continuous trains of rTMS

The pulse pattern of rTMS trains may produce different results when applied in continuous or intermittent pulse trains. For example, Rothkegel *et al.*[44] found that sub-threshold 5 Hz rTMS delivered to M1 in a continuous train of 1,200 pulses produced inhibitory neuroplastic changes in corticospinal excitability, whereas rTMS trains delivered in an intermittent fashion (also with 1,200 pulses) produced facilitation. These effects were measured using electromyographic (EMG) recordings of the targeted hand muscle's MEP; the effects of pulse pattern on the local and remote brain regions of the motor network were not investigated. In fact, we have not been able to find direct comparisons of pulse pattern effects on any targeted brain networks in any of our literature searches. Furthermore, there have been no studies demonstrating this phenomenon at supra-threshold rTMS intensities—at which many rTMS treatments are performed.[45] For example, in a supplementary experiment reported in our initial rTMS frequency study of the baboon's motor network,[8] we found no differences when 3 Hz rTMS was applied intermittently (i.e. on/off 5 second-trains) or continuously (each for a total of 150 seconds). Each rTMS pulse pattern produced similar CBF responses throughout the targeted motor network. Figure S1 of the Supplementary Materials section shows that the CBF responses at the targeted M1 site and in all of the 37 sites assessed in that study were not significantly different from each other. In addition, a very significant ($p < 0.0001$) linear relationship existed between intermittent and continuously applied rTMS-induced brain activity (see Figure S1). Therefore, we believe that (at least) at these session durations (≤150 seconds; ≤450 pulses), intermittent or continuously applied pulse trains were not as important as the rTMS frequency on the local (and/or remote) changes in CBF. As such, we are confident that the effective connectivity differences reported in this study demonstrate the frequency-dependent nature of these brain regions and are not the result of the different pulse patterns applied at certain frequencies. However, we do agree that the preliminary findings reported in this study do warrant validation—using variations of rTMS frequency, intensity, and pulse pattern—to conclusively determine if these parameters influence the effective connectivity results reported in this study.

Sub-threshold vs. supra-threshold rTMS

As TMS intensity increases, the size of the targeted site's neuronal population—i.e. excitatory and inhibitory neurons—above firing threshold also increases.[8] Several studies[46–48] have demonstrated, using EMG recordings of targeted muscles, that supra-threshold TMS intensities delivered to M1 produce a cortical silent period (CSP)—lasting up to 200 ms[47]—immediately following the muscle's MEP. In addition, increasing TMS intensity also increases the duration of the CSP[46–48]—e.g. a 120% rMT TMS pulse will have a longer CSP than a 110% rMT TMS pulse delivered at the same rTMS frequency. This effect is most likely due to the summation of inhibitory post-synaptic potentials mediated by $GABA_B$ receptors.[48] Moreover, increasing the frequency of rTMS pulses (delivered at the same supra-threshold % rMT) also increases the CSP when using rTMS frequencies ≥ 2 Hz.[47,48] Consequently, by delivering supra-threshold rTMS at high frequencies (e.g. ≥ 5 Hz) we may have biased our effective connectivity results as our rTMS frequency was increased up to 15 Hz, since each rTMS pulse delivered within the previous pulse's CSP may not have the same effect as the initial pulse. The compounded effect of high rTMS frequency and

supra-threshold intensity may explain why we observed a decrease in the functional and effective connectivity of L-M1 at higher stimulation rates (i.e. 10 Hz and 15 Hz). Therefore, further investigations—including sub-threshold rTMS intensities—may inform whether or not the frequency effects described in this study are the result of longer CSPs or if they are due to the frequency-dependence of the network.

At sub-threshold rTMS intensities, however, CBF only changes at the targeted brain site,[7,27,33] whereas supra-threshold rTMS stimulates both the local and remote nodes of the targeted brain network.[8,9,19,20,26,30,32,33,49,50] Thus, at sub-threshold rTMS intensities, we may only be able to assess frequency-dependence at the site of stimulation and not in the other nodes of the targeted brain network. Nonetheless, Siebner *et al.*[7] found that sub-threshold 5 Hz rTMS produced the largest M1 CBF changes when delivering rTMS at stimulation rates of 1–5 Hz. Therefore, we are confident that our results represent the frequency-specific predilections of the motor network since we observed 1) a network-wide increase in many of the motor network nodes at 5 Hz rTMS and 2) some nodes demonstrated their strongest path coefficients at 10 Hz and 15 Hz rTMS. These results suggest that any (potential) increases in CSP duration may not overcome the inherent frequency-dependence of the motor network.

CONCLUSIONS

We have demonstrated that 1) 5 Hz rTMS revealed the strongest path coefficients (i.e. causal influence) on the nodes of the motor network, 2) stimulation at “excitatory” rTMS frequencies did not produce increased CBF in all nodes of the motor network, and 3) specific rTMS frequencies may be used to target specific none-to-node interactions in the stimulated brain network. We would argue that this frequency dependence also exists in other brain networks (e.g. the fronto-limbic depression circuit) and more research needs to be performed to determine the optimum frequency for each brain circuit and/or node. This approach may have significant influence on the efficacy of rTMS brain therapies.

Supplementary Material

Refer to Web version on PubMed Central for supplementary material.

Acknowledgments

The study was funded by National Institute of Neurological Disorders and Stroke (NIH/NINDS; R21 NS065431, C.Á. Szabó; R21 NS062254, P.T. Fox). Dr. Salinas was supported by a Ruth L. Kirschstein National Research Service Award from the National Institute of Neurological Disorders and Stroke (NIH/NINDS F32 NS066694). The authors would like to thank Lisa Jones and Dr. Michelle Leland for performing the animal handling and sedation protocols. We would like to thank Dr. Jinqi Li and Betty Heyl for image acquisition assistance and Dr. Jack Lancaster for assistance with the rTMS/PET setup as well as enlightening discussions about rTMS.

References

1. Mayberg HS, Liotti M, Brannan SK, et al. Reciprocal limbic-cortical function and negative mood: converging PET findings in depression and normal sadness. Am J Psychiatry. 1999; 156(5):675–82. [PubMed: 10327898]
2. Mayberg HS, Lozano AM, Voon V, et al. Deep Brain Stimulation for Treatment-Resistant Depression. Neuron. 2005; 45(5):651–660. [PubMed: 15748841]

3. Fox MD, Buckner RL, White MP, et al. Efficacy of Transcranial Magnetic Stimulation Targets for Depression Is Related to Intrinsic Functional Connectivity with the Subgenual Cingulate. Biological psychiatry. 2012; 0
4. Fitzgerald PB, Fountain S, Daskalakis ZJ. A comprehensive review of the effects of rTMS on motor cortical excitability and inhibition. Clinical neurophysiology. 2006; 117(12):2584–2596. [PubMed: 16890483]
5. Pell GS, Roth Y, Zangen A. Modulation of cortical excitability induced by repetitive transcranial magnetic stimulation: Influence of timing and geometrical parameters and underlying mechanisms. Progress in Neurobiology. 2011; 93(1):59–98. [PubMed: 21056619]
6. Pascual-Leone A, Valls-Sole J, Wassermann EM, et al. Responses to rapid-rate transcranial magnetic stimulation of the human motor cortex. Brain. 1994; 117(Pt 4):847–58. [PubMed: 7922470]
7. Siebner HR, Takano B, Peinemann A, et al. Continuous transcranial magnetic stimulation during positron emission tomography: a suitable tool for imaging regional excitability of the human cortex. NeuroImage. 2001; 14(4):883–90. [PubMed: 11554807]
8. Salinas FS, Narayana S, Zhang W, et al. Repetitive Transcranial Magnetic Stimulation Elicits Rate-Dependent Brain Network Responses in Non-Human Primates. Brain Stimulation. 2013; 6(5):777–787. [PubMed: 23540281]
9. Salinas FS, Szabó CÁ, Zhang W, et al. Functional neuroimaging of the baboon during concurrent image-guided transcranial magnetic stimulation. NeuroImage. 2011; 57(4):1393–401. [PubMed: 21664276]
10. Committee for the Update of the Guide for the Care, Use of Laboratory Animals, and National Research Council. Guide for the Care and Use of Laboratory Animals. The National Academies Press; Washington, D.C: 2011.
11. Animal Welfare Act 7 U.S.C. 54 § 2143, 2009,
12. Szabó CA, Leland MM, Knape K, et al. Clinical and EEG phenotypes of epilepsy in the baboon (Papio hamadryas spp.) Epilepsy research. 2005; 65(1–2):71–80. [PubMed: 15994062]
13. Wey H-Y, Li J, Szabó CÁ, et al. BOLD fMRI of visual and somatosensory-motor stimulations in baboons. NeuroImage. 2010; 52(4):1420–7. [PubMed: 20471483]
14. Woolrich MW, Jbabdi S, Patenaude B, et al. Bayesian analysis of neuroimaging data in FSL. NeuroImage. 2009; 45(1 Suppl):S173–86. [PubMed: 19059349]
15. Smith SM, Jenkinson M, Woolrich MW, et al. Advances in functional and structural MR image analysis and implementation as FSL. NeuroImage. 2004; 23(Suppl 1):S208–19. [PubMed: 15501092]
16. Penfield W, Boldrey E. Somatic motor and sensory representation in the cerebral cortex of man as studied by electrical stimulation. Brain. 1937; 60(4):389–443.
17. Salinas FS, Lancaster JL, Fox PT. Detailed 3D models of the induced electric field of transcranial magnetic stimulation coils. Phys Med Biol. 2007; 52(10):2879–92. [PubMed: 17473357]
18. Salinas FS, Lancaster JL, Fox PT. 3D modeling of the total electric field induced by transcranial magnetic stimulation using the boundary element method. Phys Med Biol. 2009; 54(12):3631–47. [PubMed: 19458407]
19. Fox PT, Narayana S, Tandon N, et al. Column-based model of electric field excitation of cerebral cortex. Hum Brain Mapp. 2004; 22(1):1–14. [PubMed: 15083522]
20. Fox P, Ingham R, George MS, et al. Imaging human intra-cerebral connectivity by PET during TMS. Neuroreport. 1997; 8(12):2787–91. [PubMed: 9295118]
21. Peinemann A, Reimer B, Löer C, et al. Long-lasting increase in corticospinal excitability after 1800 pulses of subthreshold 5 Hz repetitive TMS to the primary motor cortex. Clinical neurophysiology. 2004; 115(7):1519–1526. [PubMed: 15203053]
22. Nettekoven C, Volz LJ, Kutscha M, et al. Dose-Dependent Effects of Theta Burst rTMS on Cortical Excitability and Resting-State Connectivity of the Human Motor System. The Journal of neuroscience: the official journal of the Society for Neuroscience. 2014; 34(20):6849–6859. [PubMed: 24828639]

23. Jenkinson M, Bannister P, Brady M, et al. Improved optimization for the robust and accurate linear registration and motion correction of brain images. NeuroImage. 2002; 17(2):825–41. [PubMed: 12377157]
24. Lancaster JL, Fox PT, Downs H, et al. Global spatial normalization of human brain using convex hulls. J Nucl Med. 1999; 40(6):942–55. [PubMed: 10452309]
25. Lee L, Siebner HR, Rowe JB, et al. Acute remapping within the motor system induced by low-frequency repetitive transcranial magnetic stimulation. J Neurosci. 2003; 23(12):5308–18. [PubMed: 12832556]
26. Speer AM, Willis MW, Herscovitch P, et al. Intensity-dependent regional cerebral blood flow during 1-Hz repetitive transcranial magnetic stimulation (rTMS) in healthy volunteers studied with H215O positron emission tomography: I. Effects of primary motor cortex rTMS. Biological psychiatry. 2003; 54(8):818–25. [PubMed: 14550681]
27. Rounis E, Lee L, Siebner HR, et al. Frequency specific changes in regional cerebral blood flow and motor system connectivity following rTMS to the primary motor cortex. NeuroImage. 2005; 26(1): 164–76. [PubMed: 15862216]
28. Saleem, KS., Logothetis, NK. A combined MRI and histology atlas of the rhesus monkey brain in stereotaxic coordinates. Academic Press; London: 2007.
29. Arbuckle, JL. Amos (version 7.0)[computer program]. Chicago: SPSS; 2006.
30. Laird AR, Robbins JM, Li K, et al. Modeling motor connectivity using TMS/PET and structural equation modeling. NeuroImage. 2008; 41(2):424–36. [PubMed: 18387823]
31. Price LR, Tulsky D, Millis S, et al. Redefining the factor structure of the Wechsler Memory Scale-III: Confirmatory factor analysis with cross-validation. Journal of Clinical and Experimental Neuropsychology. 2002; 24(5):574–585. [PubMed: 12187442]
32. Paus T, Jech R, Thompson CJ, et al. Transcranial magnetic stimulation during positron emission tomography: a new method for studying connectivity of the human cerebral cortex. The Journal of neuroscience. 1997; 17(9):3178–84. [PubMed: 9096152]
33. Bestmann S, Baudewig J, Siebner HR, et al. Subthreshold high-frequency TMS of human primary motor cortex modulates interconnected frontal motor areas as detected by interleaved fMRI-TMS. NeuroImage. 2003; 20(3):1685–96. [PubMed: 14642478]
34. Fox PT, Narayana S, Tandon N, et al. Intensity modulation of TMS-induced cortical excitation: primary motor cortex. Hum Brain Mapp. 2006; 27(6):478–87. [PubMed: 16161021]
35. Narayana S, Laird AR, Tandon N, et al. Electrophysiological and functional connectivity of the human supplementary motor area. NeuroImage. 2012; 62(1):250–265. [PubMed: 22569543]
36. Dum RP, Strick PL. Motor areas in the frontal lobe of the primate. Physiology & behavior. 2002; 77(4–5):677–82. [PubMed: 12527018]
37. Dum RP, Strick PL. Frontal lobe inputs to the digit representations of the motor areas on the lateral surface of the hemisphere. The Journal of neuroscience. 2005; 25(6):1375–86. [PubMed: 15703391]
38. Vasant DH, Michou E, Mistry S, et al. High-frequency focal repetitive cerebellar stimulation induces prolonged increases in human pharyngeal motor cortex excitability. The Journal of Physiology. 2015; 593(22):4963–4977. [PubMed: 26316351]
39. Seminowicz DA, Mayberg HS, McIntosh AR, et al. Limbic-frontal circuitry in major depression: a path modeling metanalysis. NeuroImage. 2004; 22(1):409–418. [PubMed: 15110034]
40. Chen R, Gerloff C, Classen J, et al. Safety of different inter-train intervals for repetitive transcranial magnetic stimulation and recommendations for safe ranges of stimulation parameters. Electroencephalography and clinical neurophysiology. 1997; 105(6):415–21. [PubMed: 9448642]
41. Wey H-Y, Wang DJ, Duong TQ. Baseline CBF, and BOLD, CBF, and CMRO(2) fMRI of visual and vibrotactile stimulations in baboons. Journal of cerebral blood flow and metabolism. 2011; 31(2):715–24. [PubMed: 20827260]
42. Szabó CA, Narayana S, Franklin C, et al. “Resting” CBF in the epileptic baboon: correlation with ketamine dose and interictal epileptic discharges. Epilepsy research. 2008; 82(1):57–63. [PubMed: 18801644]
43. Szabó CA, Salinas FS, Narayana S. Functional PET evaluation of the photosensitive baboon. OPEN Neuroscience Journal. 2011; 5:206–15.

44. Rothkegel H, Sommer M, Paulus W. Breaks during 5Hz rTMS are essential for facilitatory after effects. Clinical neurophysiology. 2010; 121(3):426–430. [PubMed: 20006546]

45. Lefaucheur JP, Andre-Obadia N, Antal A, et al. Evidence-based guidelines on the therapeutic use of repetitive transcranial magnetic stimulation (rTMS). Clinical neurophysiology : official journal of the International Federation of Clinical Neurophysiology. 2014; 125(11):2150–206. [PubMed: 25034472]

46. Berardelli A, Inghilleri M, Gilio F, et al. Effects of repetitive cortical stimulation on the silent period evoked by magnetic stimulation. Experimental Brain Research. 1999; 125(1):82–86. [PubMed: 10100980]

47. Romeo S, Gilio F, Pedace F, et al. Changes in the cortical silent period after repetitive magnetic stimulation of cortical motor areas. Experimental brain research. 2000; 135(4):504–510. [PubMed: 11156314]

48. Daskalakis ZJ, Möller B, Christensen BK, et al. The effects of repetitive transcranial magnetic stimulation on cortical inhibition in healthy human subjects. Experimental Brain Research. 2006; 174(3):403–412. [PubMed: 16683138]

49. Sack AT, Kohler A, Bestmann S, et al. Imaging the Brain Activity Changes Underlying Impaired Visuospatial Judgments: Simultaneous fMRI, TMS, and Behavioral Studies. Cerebral cortex. 2007; 17(12):2841–2852. [PubMed: 17337745]

50. Bestmann S, Ruff CC, Blakemore C, et al. Spatial Attention Changes Excitability of Human Visual Cortex to Direct Stimulation. Current Biology. 2007; 17(2):134–139. [PubMed: 17240338]

Highlights

- 1st study to investigate the rate-dependence of effective connectivity in the motor network with rTMS
- 5 Hz rTMS revealed the strongest path coefficients (i.e. causal influence) on the nodes of the motor network
- Stimulation at “excitatory” rTMS frequencies did not produce increased CBF in all nodes of the motor network
- Specific rTMS frequencies may be used to target specific none-to-node interactions in the stimulated brain network
- We propose that specific brain circuits may be targeted not only by their anatomical location, but also by the frequency-dependence of that brain network’s nodes

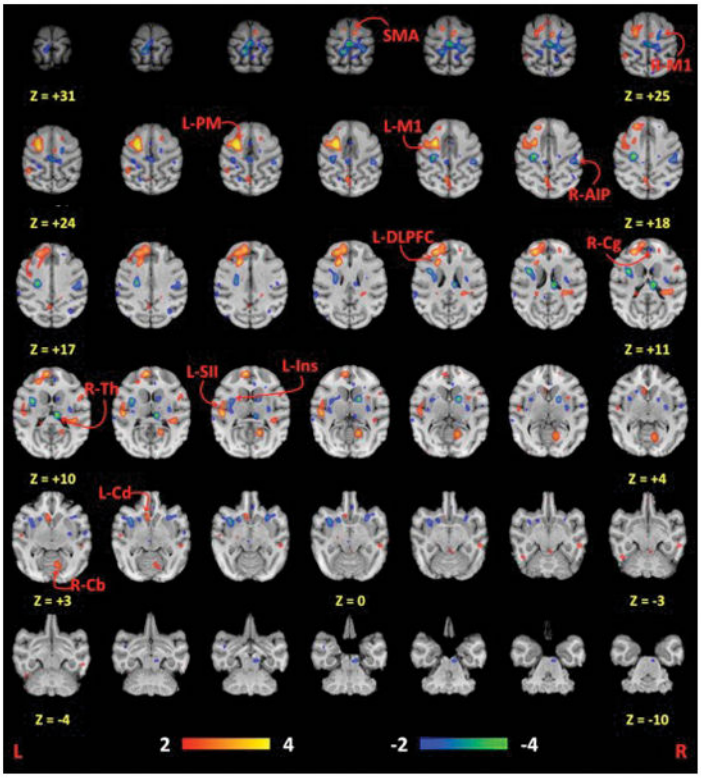

Figure 1.

Statistical parametric images of all rTMS frequencies compared to rest. All coordinates are relative to the anterior commissure, which is located at (0 mm, 0 mm, 0 mm). L = Left; R = Right; M1 = primary motor cortex; PM = dorsal premotor cortex; SMA = supplementary motor area; Cg = cingulate motor area; Cd = caudate; Th = thalamus; Cb = cerebellum; DLPFC = dorsolateral prefrontal cortex; Ins = insular cortex; SII = parietal operculum; AIP = anterior intraparietal sulcus. Image reprinted with permission from Elsevier and Salinas *et al.*.[8]

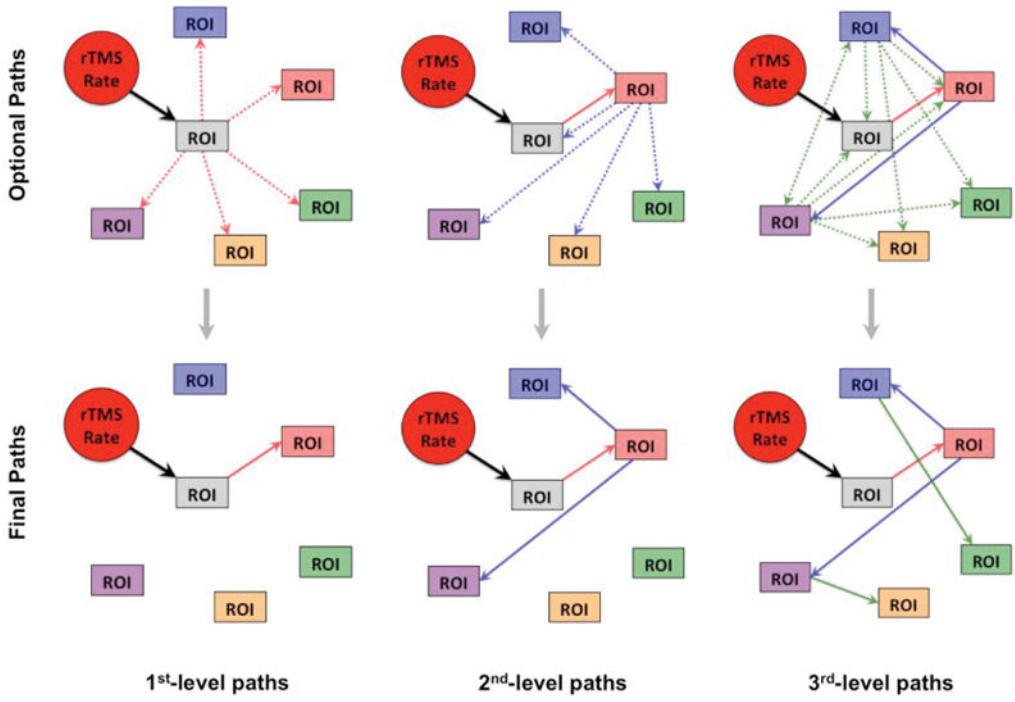

Figure 2. Path analysis

Beginning with the required path of rTMS rate loading onto the targeted (i.e. gray) region-of-interest (ROI), the path analysis procedure then assesses which of the "optional paths" (top) are most probable due the covariance of the data; this results in a "final path" (bottom) for that first-level of path analysis. Once determined, the first-level path (red path) is then set as a required path, along with the rTMS rate loading on the target ROI, and the next level of optional path loadings (blue paths) are then modeled from the first level node. This procedure is repeated until the addition of more path levels (green paths, etc.) does not improve the fit of the model, resulting in a final model of the effective connectivity of the stimulated brain network.

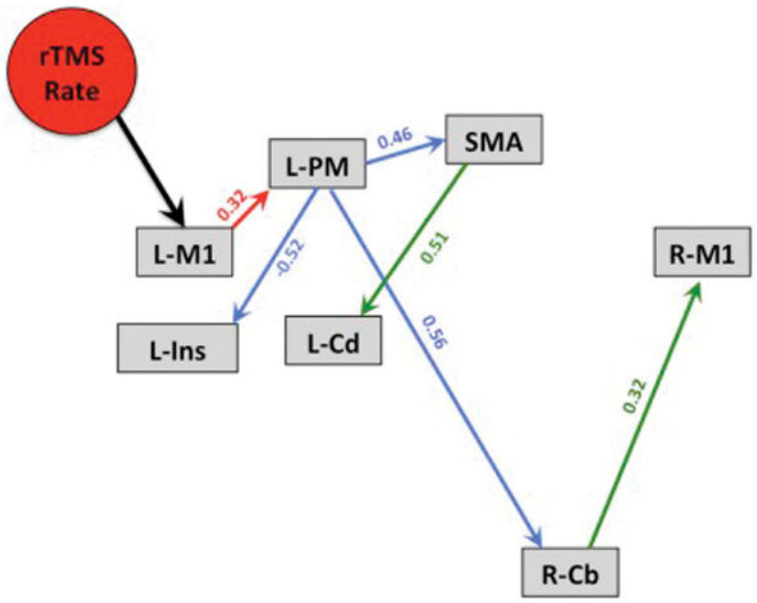

Figure 3. Final model of L-M1 effective connectivity

Exploratory path analysis revealed that seven nodes produced a very well fitting model of the effect of rTMS rate on the motor network. Red paths = 1st-level path; blue paths = 2nd-level paths; green paths = 3rd-level paths.

Table 1

Regions of brain activity during rTMS compared to the baseline condition (N = 5).

Region of Interest	Area*	Label	Coordinates** (mm)			Volume (mm^3)	*Z* score	*p* value
			x	y	z			
§ Dorsal precentral	F1	L-M1	−19	−1	20	680	3.13	0.0007
Dorsal precentral	F1	R-M1	9	−7	25	568	−2.84	0.0023
Dorsal premotor	F2	L-PM	−13	0	22	1000	5.04	$p<0.00003$
Superior frontal gyrus	SMA	SMA	3	5	28	560	2.97	0.0015
Anterior cingulate cortex	Area 24b	R-Cg	3	15	11	328	−2.46	0.0069
Cerebellum	Cblm	R-Cb	21	−18	3	872	3.01	0.0013
Caudate nucleus	-	L-Cd	−4	11	2	712	2.97	0.0015
Thalamus	-	R-Th	5	−13	10	992	−4.56	$p<0.00003$
Parietal operculum	SII	L-SII	−26	−4	8	664	2.79	0.0027
Insular cortex	Ial	L-Ins	−19	7	1	880	−3.18	0.0007
Anterior intraparietal sulcus	AIP	R-AIP	23	−16	19	864	−2.96	0.0015

*Labels correspond to the homologous areas listed in the rhesus[28]

**Coordinates are relative to the anterior commissure (0 mm, 0 mm, 0 mm)

§Targeted primary motor cortex

Table 2

Fit statistics of the model in each level of path analysis (N = 5).

	χ^2	χ^2-df	BCC(0)	BIC(0)	χ^2/df	p
First-level paths	50.0354	24.035	0.000	0.000	1.924	0.003
Second-level paths	31.0286	8.0286	0.000	0.000	1.349	0.122
Third-level paths	18.040	−2.960	0.000	0.000	0.859	0.647

Table 3

Path coefficients of each pathway at each rTMS frequency (N = 5).

Pathway			3Hz		5Hz		10Hz		15Hz	
			Path Coeff.	**p**	**Path Coeff.**	**p**	**Path Coeff.**	**p**	**Path Coeff.**	**p**
L-M1	←	Rate	0.398	0.045	0.425	0.004	0.164	0.011	0.156	p < 0.001
Premotor	←	L-M1	0.271	0.359	0.661	p < 0.001	0.531	0.001	0.437	0.018
SMA	←	Premotor	0.486	0.041	0.768	0.003	0.638	0.005	0.625	p < 0.001
Cerebellum	←	Premotor	0.931	0.025	0.275	0.491	1.110	0.003	0.820	0.022
Insula	←	Premotor	−0.611	0.011	−0.718	0.006	−0.361	0.190	−0.323	0.219
Caudate	←	SMA	0.703	0.025	0.620	p < 0.001	0.426	0.051	0.724	0.005
R-M1	←	Cerebellum	0.060	0.618	0.032	0.853	0.283	0.126	0.265	0.209